Driver Warning Strategies for a Critical Cornering Maneuver

Matthijs KLOMP*
Saab Automobile, Vehicle Dynamics
Trollhättan, Sweden

Jonas BILLBERG and Andreas DOUHAN
Royal Institute of Technology
Division of Vehicle Dynamics
Stockholm, Sweden

Abstract

The hypothesis in this paper is that the involvement of the driver in mitigating vehicle instability would require less intervention from the active system and also provide faster stabilization. Several indicators of instability during a lane-change type maneuver are developed to support a driver warning. First the focus is on indicators which are related to variables which are measured in vehicles equipped with stability control (ESC) systems. These indicators could trigger a warning for which the driver would have around one second to take corrective action. These indicators are compared to classical evaluation tools such as the moment method, phase portrait analysis and Lyapunov analysis. This preliminary theoretical study suggests that stability indicators based on side-slip rate and yaw acceleration could give an early indication of possible instability. An example is also given which shows that a combination of countersteer and ESC intervention triggered a quicker ESC intervention with a shorter duration. This illustrates how a cooperation between the driver and the ESC system could give a better driver/vehicle system performance.

---

*Corresponding author. e-mail: `matthijs.klomp@saab.com`

1   Introduction

Drivers operate most of time driving a vehicle in the linear range of the tires
and they are accustomed to the vehicle's response in that region. However,
on low-friction surfaces or during emergency maneuvers, the sometimes dras-
tically changed vehicle response in the non-linear range is unanticipated by
most drivers and may result in loss of control.

The possible loss of control in the nonlinear range of operation may be
due to either loss of maneuverability (unable to track a desired path) or loss
of lateral stability (unable to stabilize the vehicle motion). Even though
these critical situations would be avoided with the intervention by electronic
stability control (ESC) systems [10] it is desirable that, if possible, the driver
should be warned prior to such an intervention. The hypothesis here is that
the involvement of the driver in mitigating vehicle instability would require
less intervention from the active system and also provide faster stabilization.

In order to issue a useful driver warning, it is necessary to

1. determine which factors indicate a critical cornering maneuver,

2. decide on an appropriate driver correction,

3. warn (and instruct) the driver, and

4. avoid false warnings.

It is also essential to evaluate the effectiveness and quantify the driver cor-
rection necessary to mitigate the critical situation.

In the literature, valuable contributions for the assessment of loss of con-
trol accidents are described in [5] and [2], where both discrete and contin-
uous stability indexes are used to evaluate how critical a given maneuver
is. The stability index in [5] is mainly based on deviations of the measured
yaw rate from that of a reference model. Moreover, the work is focused on
post-accident analysis. In [2] instead, the grip limit and a prediction of the
future utilized grip is used as thresholds for driver warning. The warning
thresholds in this work are based on similar principles as described in [5]
and [2], but here their work will be expanded by applying them to real-time
monitoring of the vehicle maneuvering. One other common method to deter-
mine insufficient maneuverability or stability is to relate to the deviation of
the actual from desired vehicle motion [4, 11, 18]. This method is typically
used to trigger a brake intervention by an ESC system. With this method,
loss of maneuverability is defined such that vehicle yaw rate is less than the
reference yaw rate. Loss of stability is defined as a too high yaw rate and

loss of maneuverability is indicated by insufficient yaw rate relative to the desired/reference yaw rate

The objective of this paper is to perform a preliminary theoretical investigation on possible indicators of instability for one specific type of maneuver. Additionally, the effect of a stabilization intervention from the driver (countersteer) is studied with and without cooperation of the ESC system. The robustness evaluation of the indicators is limited to two different friction levels and two different vehicle speeds.

This paper is organized such that first in Sec. 2 different methods that have been used for driver warning are discussed and how fast the driver might react to a particular warning. In Sec. 3 the model to be used for subsequent simulation studies is described. Further a reference model and deviation from this model is described. Here the stability control and friction estimation is introduced that will be used for the warning evaluation and warning indicators, respectively. In Sec. 4 a critical cornering maneuver is described and how to assess this maneuver in relation to stability and maneuverability. The cornering limits of a vehicle are analyzed by studying the static directional stability and control of the vehicle related to the Milliken moment method [12]. Further warning indicators that could be used for driver warning are determined in Sec. 5. These warning indicators are evaluated in Sec. 6 together with a subsequent driver correction with and without ESC control. In Sec. 7 the findings are summarized and future work is indicated.

2 Driver Warning Strategies

In order to warn the driver, using criteria developed in this work, more work outside the scope of this paper is required to find the correct method to design a driver warning system. The purpose of this section is to give some discussion on methods proposed in the literature. A warning that catches the driver's attention is essential but more important is how the driver reacts to the warning. If the warning is easy to detect, but the driver reacts incorrectly, the warning can instead have a negative outcome. Krausman et al. [9] have found that humans have the shortest reaction time when exposed to tactile stimuli. They also found that human reacts slowest to visual alerts but that the most efficient in getting attention was visual together with auditory alert. Comparing auditory warnings with visual warnings the auditory warning have an alerting advantage over visual warnings in that drivers are not required to look at the display to perceive the warning [15].

According to [16] drivers were less annoyed when exposed to haptic warnings compared to visual and auditory warnings. It is also stated that auditory

combined with visual warnings enhance performance and reduce time to respond to information. Participants in [16] tended to rely on auditory and haptic cues and used the visual cue as a confirmation only. Reaction time was slower when exposed to a haptic + auditory warning compared to a haptic alone.

The driver's reaction is essential for the warning strategy and the indicators that are developed. In [17] the reaction time has been evaluated with both anticipated and unanticipated warning. In this matter the unpredicted warning is the one of interest since the driver will not be aware of the upcoming situation. The reaction time for the unpredicted warning was 0.52s when the warning was delivered through a steering vibration, 0.72s with a pulse like steering torque, 1.19s with a monaural beep sound warning and 1.36s with a stereo beep sound [17].

Based on indications in [17] it is therefore assumed that the driver must be warned at least 0.5s and preferably around 1s prior to a driver correction being necessary.

3 Vehicle Modeling, Stability Control and Friction Estimation

The vehicle model used for simulations is shown in Fig. 1. This vehicle is a front-steered vehicle with parallel steering on the left and right wheels. The longitudinal forces are assumed to be individually controllable, which will be utilized in a simple ESC control described later in this section.
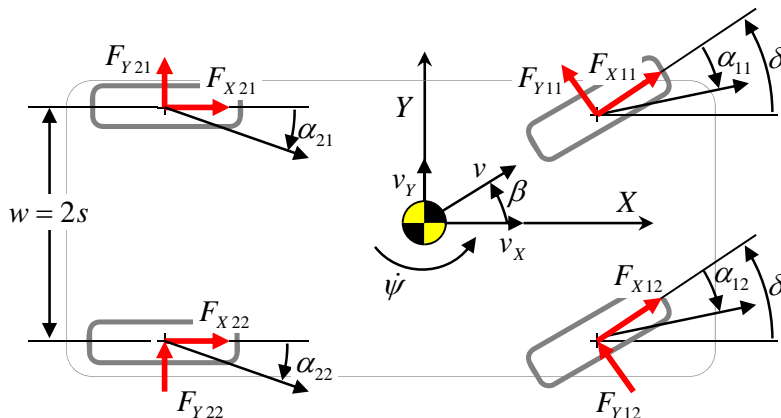
Figure 1: Two Track Vehicle Model

3.1 Two-Track Vehicle Model

In the described vehicle model, only the planar motion of the vehicle is considered, i.e. the longitudinal, lateral and yaw velocities are chosen as state variables v_X, v_Y and $\dot{\psi}$, respectively. This means that other dynamics of the vehicle, such as roll, pitch, wheel rotation, steering system and driveline dynamics, are neglected. A discussion on some of these assumptions can be found in [19], where the conclusion is that the planar dynamics and tire non-linearities are the most important factors to consider for most maneuvers. The vehicle data used in this paper and subsequent analysis is given in App. A. From Newton's second law of motion the following state-space model can be derived:

$$
\begin{bmatrix} \dot{v}_X \\ \dot{v}_Y \\ \ddot{\psi} \end{bmatrix} = \begin{bmatrix} m & 0 & 0 \\ 0 & m & 0 \\ 0 & 0 & mk^2 \end{bmatrix}^{-1} \begin{bmatrix} 1 & 1 & 1 & 1 \\ \delta & \delta & 0 & 0 \\ (\delta l_1 - s) & (\delta l_1 + s) & -s & s \end{bmatrix} \mathbf{q}_X
$$

$$
+ \begin{bmatrix} m & 0 & 0 \\ 0 & m & 0 \\ 0 & 0 & mk^2 \end{bmatrix}^{-1} \begin{bmatrix} -\delta & -\delta & 0 & 0 \\ 1 & 1 & 1 & 1 \\ l_1 & l_1 & -l_2 & -l_2 \end{bmatrix} \mathbf{q}_Y + \begin{bmatrix} v_Y \dot{\psi} \\ -v_X \dot{\psi} \\ 0 \end{bmatrix} \quad (1)
$$

$$
- \begin{bmatrix} \zeta g + 1/2 \rho C_D A_f v_X |v_X|/m \\ 0 \\ 0 \end{bmatrix} = \mathbf{f}(\mathbf{x}, \mathbf{u}) ,
$$

where m is the vehicle mass, k the radius of gyration and where the longitudinal and lateral forces, $\mathbf{q}_X$ and $\mathbf{q}_Y$, respectively, are

$$
\mathbf{q}_X = \begin{bmatrix} F_{X11} & F_{X12} & F_{X21} & F_{X22} \end{bmatrix}^\top ,
$$
$$
\mathbf{q}_Y = \begin{bmatrix} F_{Y11} & F_{Y12} & F_{Y21} & F_{Y22} \end{bmatrix}^\top , \quad (2)
$$

and where the state vector, $\mathbf{x}$, and the control input vector, $\mathbf{u}$, are

$$
\mathbf{x} = \begin{bmatrix} v_X & v_Y & \dot{\psi} \end{bmatrix}^\top ,
$$
$$
\mathbf{u} = \begin{bmatrix} \delta & \mathbf{q}_X^\mathrm{T} \end{bmatrix}^\top ; , \quad (3)
$$

i.e. $\mathbf{u}$ is the control input vector containing the steering angle, δ, and the longitudinal forces F_{Xij}.

The normal forces, F_{Zij}, acting on each wheel are given by the static load distribution and the longitudinal and lateral load transfer. This load transfer is due to longitudinal and lateral acceleration, denoted a_X and a_Y, respectively. The normal forces can be derived to be

$$
F_{Zij} = m((l-l_i)g + (-1)^i h a_X)/(2l) + (-1)^j \zeta_i m a_Y, \quad i = 1, 2, \quad j = 1, 2, \quad (4)
$$

where ζ_i is the lateral load transfer coefficient of each axle, g is the gravitational acceleration and h is the height of the center of mass above the ground and where

$$
\begin{aligned}
a_X &= \dot{v}_X - v_Y \dot{\psi}, \\
a_Y &= \dot{v}_Y + v_X \dot{\psi}.
\end{aligned}
\tag{5}
$$

For more details on the normal force distribution in (4), see [8, 14].

The lateral forces, $\mathbf{q}_Y$ can be modeled as function of the tire slip angles on each wheel, α_{ij}, the longitudinal forces F_{Xij} and normal forces F_{Zij} by using the well-known Magic tire model [14], where

$$
F_Y = D \sin(C \arctan(B\alpha - E(B\alpha - \arctan(B\alpha)))),
\tag{6}
$$

using tire data given in App. A. The slip angles, α_{ij}, are related to the longitudinal, lateral and yaw velocity at the center of gravity as

$$
\alpha_{ij} = \arctan \frac{v_{Y_{Wij}}}{|v_{X_{Wij}}|} = \delta_{ij} - \arctan\left(\frac{v_Y + (-1)^{i+1} l_i \dot{\psi}}{|v_X + (-1)^j s\dot{\psi}|} \right), \quad i = 1, 2, \quad j = 1, 2,
\tag{7}
$$

since the slip angle is the angle between direction of the tire velocity vector and the free rolling direction using the definition in [14]. The local wheel velocities, V_{X_W} and V_{Y_W}, are obtained by transforming the velocities of the center of mass to each tire contact point.

3.2   Reference Model

As stated in the introduction, it is common to model the desired vehicle characteristics with the yaw-rate response of a linear bicycle model to the steering input from the driver [4]. The reference yaw rate is derived by integrating the following simple bicycle model with steering wheel angle as input and the longitudinal speed assumed to be a known slowly varying parameter

$$
\begin{bmatrix} \dot{v}_Y^{\text{ref}} \\ \ddot{\psi}^{\text{ref}} \end{bmatrix} = - \begin{bmatrix} \dfrac{C_{\alpha 1} + C_{\alpha 2}}{m v_X} & \dfrac{l_1 C_{\alpha 1} - l_2 C_{\alpha 2}}{m v_X} + v_X \\ \dfrac{l_1 C_{\alpha 1} - l_2 C_{\alpha 2}}{m k^2 v_X} & \dfrac{l_1^2 C_{\alpha 1} + l_2^2 C_{\alpha 2}}{m k^2 v_X} \end{bmatrix} \begin{bmatrix} v_Y^{\text{ref}} \\ \dot{\psi}^{\text{ref}} \end{bmatrix} + \begin{bmatrix} \dfrac{C_{\alpha 1}}{m} \\ \dfrac{l_1 C_{\alpha 1}}{m k^2} \end{bmatrix} \delta \, .
\tag{8}
$$

where $C_\alpha = BCD$ according to parameters in App. A. The reference yaw rate is limited to that which is attainable on a dry surface. The reference yaw rate is therefore limited to be no more than

$$
|\dot{\psi}^{\text{ref}}| \leq \frac{\bar{a}_Y - |\dot{v}_Y|}{v_X} \, ,
\tag{9}
$$

where $\bar{a}_Y$ is some pre-determined maximum steady-state lateral acceleration.

3.3 Model Reference Deviation

The yaw rate error is deviation of the measured actual yaw rate from the reference yaw rate. In general, larger yaw rate than the reference yaw rate is an indication of instability, often referred to as oversteer. Less yaw rate relative to the reference yaw rate is instead an indication of loss of manueverability, referred to as understeer.

Here, a combination of two different definitions of the yaw rate error, e, are used

$$e_1 = (\dot{\psi} - \dot{\psi}^{\text{ref}})\text{sign}(\dot{\psi}) \tag{10}$$

$$e_2 = |\dot{\psi}| - |\dot{\psi}^{\text{ref}}| \tag{11}$$

where a positive error indicates oversteer and a negative error indicates understeer. It is here proposed to introduce the yaw rate error as

$$e = \gamma e_1 + (1 - \gamma)e_2 \ , \tag{12}$$

where $0 \leq \gamma \leq 1$ is a tuning parameter that determines the desired balance between the two yaw rate error definitions, e_1 and e_2. In most cases $e_1 = e_2$, but not when the actual and reference yaw rate have opposite sign, i.e. $\dot{\psi}\dot{\psi}^{\text{ref}} < 0$. This usually occurs when the driver countersteers in an oversteer situation and the reference model changes yaw rotation direction before the actual vehicle does. One of the decisions one has to make is how to interpret the driver's intention in this case. One reasonable interpretation of the countersteer is that the driver herself takes the correct action and countersteers to stabilize the vehicle. In this case e_1 increases and e_2 decreases. The tuning parameter γ is introduced to determine how much countersteering by the driver should influence the intervention of the ESC system.

3.4 Stability Control by Braking (ESC)

The ESC strategy used in this paper is a simple proportional brake controller which is activated when the yaw rate error, e given by (12), violates a predetermined threshold. When exceeding an upper threshold of the error, an "oversteer" intervention is activated. Conversely, violating a lower threshold triggers an "understeer" intervention. After activation the stability control is deactivated again when e has decreased to be below half the activation threshold. This hysteresis in the control is added to avoid switching of the control around the activation threshold. The algorithm of the simple stability control used here is

if $e > \bar{e}$ or $(e > \bar{e}/2$ and $\epsilon = 1)$ **then** {Oversteer control}

$\epsilon = 1$

$\mathbf{q}_X = -K_{P1}|e| \begin{bmatrix} \dot{\psi} < 0, & \dot{\psi} > 0, & 0, & 0 \end{bmatrix}^{\mathrm{T}}$

else if $e < \underline{e}$ or $(e < \underline{e}/2$ and $\epsilon = 1)$ **then** {Understeer control}

$\epsilon = 1$

$\mathbf{q}_X = -K_{P2}|e| \begin{bmatrix} 0, & 0, & \dot{\psi} > 0, & \dot{\psi} < 0 \end{bmatrix}^{\mathrm{T}}$

else {No control}

$\epsilon = 0$

end if

In the example algorithm above, the oversteer conditions are checked first. The oversteer control is activated when e exceeds a threshold $\bar{e}$. In order to indicate that the control is active a flag ϵ is set high ($\epsilon = 1$) and the control is subsequently kept active until $e \leq \bar{e}/2$. The control itself applies a brake force on the outer front wheel proportional to the yaw rate error, with K_{P1} as the proportional gain. In this work, the understeer control is only activated on low-μ surfaces where the maneuverability criteria in [13] cannot be met without this control. Other than this, the understeer control works similar to the oversteer control and is activated when e is below a threshold value $\underline{e}$ and brakes the inner rear wheel proportional to the error with K_{P2} as the gain. When none of the conditions are met, the stability control is deactivated, ϵ is set low ($\epsilon = 0$). Preventing wheel locking by means of slip control is usually also part of an ESC implementation [4], but is omitted here for sake of brevity.

3.5 Friction estimation

The friction, μ, is simply estimated based on the maximum utilized friction within a predetermined window, ϖ. The discrete time version of the friction estimation algorithm is

if $|a_{Y_p}|/g > \hat{\mu}_{p-1}$ or $\tau_{p-1} > \varpi$ **then**

$\hat{\mu}_p = \max(|a_{Y_p}|/g, \underline{\mu})$

$\tau_k = 0$

else

$\hat{\mu}_p = \max(\hat{\mu}_{p-1}, \underline{\mu})$;

$\tau_p = \tau_{p-1} + \Delta t$

end if

Here the current time step is denoted p and the sampling time Δt. In order to avoid numerical issues, if the measured lateral acceleration within the current time window is less than a prescribed minimum lateral acceleration, the friction estimation is limited to some minimum value, $\underline{\mu}$. The results of the friction estimation algorithm can be seen in Fig. 2.

8
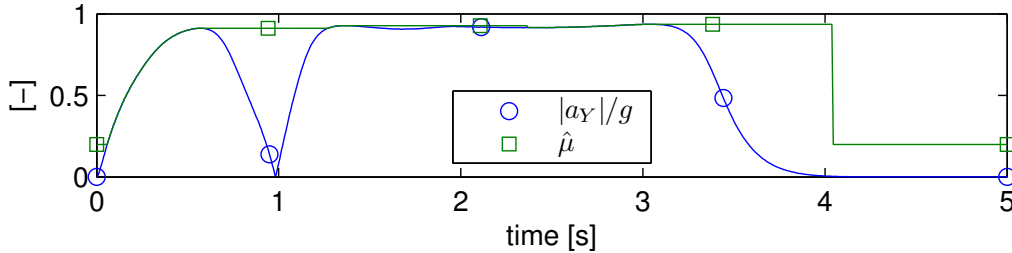
Figure 2: Friction estimation results based on lateral acceleration data from a sine-with-dwell maneuver with a steering wheel amplitude of 130°. The time window for the estimation is $\varpi = 1$s.

4   Assessment of Cornering Situation

In a highly dynamic maneuver, such as a lane-change maneuver, the steering may be cycled from one direction to the other. This rapid cycling or reversal of steering with an high amplitude is significantly different from a monotonically increasing steering input. The main difference is that at the moment the steering is reversed, the front and rear tires lateral forces have opposite sign and thereby generating an excessive yaw moment. This large yaw moment can cause the rear tires to saturate and may lead to loss of stability. Different methods which indicate a loss of stability during a sine with dwell steering reversal maneuver from the FMVSS-126 regulation [13] will here be assessed.

4.1   Dynamic Stability Criteria

The FMVSS-126 regulation requires the yaw rate to converge back to zero "fast enough" after completion of the maneuver at $t > T_0$. Here T_0 is the time where the maneuver is completed, i.e. the steering wheel input is zero. The convergence is evaluated at $t = T_0 + 4/4$ and $t = T_0 + 7/4$ after the completion of the steering maneuver, see Fig. 3.b. The maneuver passes the FMVSS stability requirements if

$$\dot{\psi}(T_0 + 4/4) < 7/20 \cdot \dot{\psi}_{\text{Peak}} \quad \text{and} \quad \dot{\psi}(T_0 + 7/4) < 4/20 \cdot \dot{\psi}_{\text{Peak}} , \qquad (13)$$

where $\dot{\psi}_{\text{Peak}}$ is the maximum absolute yaw rate during the maneuver.

Next, the stability criteria in the FMVSS-126 regulation is related to classic concepts such as exponential stability or Lyapunov stability of equilibrium points (i.e. roots of $\mathbf{f}(\mathbf{x}, \mathbf{u}) = 0$) [7]. In the present case, the equilibrium solution which is studied is $\mathbf{x} = \begin{bmatrix} v_X(t > T_0) & 0 & 0 \end{bmatrix}^{\text{T}}$ with $\mathbf{u} = 0$.

9

In order to relate the solutions to the region of attraction of a particular equilibrium point(s) it is here proposed to use a Lyapunov positive definite function $V(\mathbf{x})$ such that

$$
\begin{aligned}
V(0) &= 0, \\
V(\mathbf{x}) &> 0, \qquad \forall \mathbf{x} \neq 0.
\end{aligned}
\tag{14}
$$

Since it is of interest to relate the stability of the vehicle to the yaw/side-slip characteristics of the vehicle, it is natural to choose the yaw rate and side-slip as variables for our Lyapunov candidate function. The proposed Lyapunov candidate function is therefore

$$
V = (\dot{\psi}^2 + (\eta\beta)^2)/2,
\tag{15}
$$

which fulfills the criteria in (14). Here η is a tuning parameter determining the desired relationship between $\dot{\psi}$ and β such that solutions where $\dot{V} < 0$ are stable according to some requirements. It was found that for vehicle parameters used in this work, if $\eta = 5/2$ and the point where the β-$\dot{\psi}$ trajectory crosses the level curve

$$
\dot{V} = \dot{\psi}\ddot{\psi} + \eta^2\beta\dot{\beta} = 0 ,
\tag{16}
$$

will also violate the FMVSS-126 stability requirements in (13). If the maneuver is stable in the Lyapunov sense (i.e. $\dot{V} < 0 \quad \forall t > T_0$), the FMVSS-126 stability requirements are satisfied for some particular η.

It is known from linear systems theory that if a linear system is exponentially stable if and only if the system has negative real eigenvalues. For non-linear systems, like our vehicle, only stability of a solution or set of solutions can be studied and exponential stability cannot be guaranteed for arbitrary solutions [7]. Here the solution is compared to a given solution to the sine-with-dwell test with a known exponential

$$
g(\tau) = c_1 \exp(c_2 t), \quad \tau > T_0,
\tag{17}
$$

such that $g(T_0) = \dot{\psi}_{\text{Peak}}$ and $g(T_0 + 4/4) = 7/20 \cdot \dot{\psi}_{\text{Peak}}$. If the solution is within the boundary defined by $g(t)$ it can be concluded that the solution is exponentially stable in relation to the FMVSS-126 stability requirements (see also Fig. 5.a).

4.2   Static Cornering Limits

Three factors that determine the cornering capability of the vehicle are the lateral grip, maneuverability and stability limits. In this section measures that relate these capabilities with the grip of the front and rear axle are

established. Here an approach from [12] is used to study the directional steering control and stability from the perspective of yaw moment control available to the driver through the steering input. These measures will be used to assess vehicle stability and maneuverability for a particular maneuver.

The lateral grip margin is here defined as the normalized distance from the current lateral acceleration to the maximum lateral acceleration, or lateral grip, $\bar{a}_Y$. If the friction on the front and rear axles are known, the lateral grip utilization is defined as

$$\Xi = 1 - \left| \frac{a_Y}{\bar{a}_Y} \right| = 1 - \left| \frac{a_Y}{\min(\mu_1, \mu_2)g} \right| . \tag{18}$$

The maneuverability is defined in [6] as how many degrees the steering can be increased, while keeping the side-slip angle constant, until the front tire saturates. Similarly the maneuverability in this work is defined as how much turn-in yaw moment can be applied from the present state (side-slip constant). If steering is the only actuator available to create a turn-in moment, the maximum turn-in moment is limited by the remaining grip of the front axle. This means that it is possible to define the maneuverability margin as

$$\Phi = 1 - \left| \frac{F_{Y1}}{D_{Y1}} \right| = 1 - \left| \frac{a_Y + (k^2/l_2)\ddot{\psi}}{\mu_1 g} \right| , \tag{19}$$

i.e. the normalized distance of the front axle lateral force F_{Y1} to the maximum attainable front axle lateral force, D_{Y1}.

The grip of the rear axle is essential to stabilize the vehicle in case of a disturbance. A static stability margin can be defined as how much the side-slip can be increased, while keeping the steering constant, before the rear axle saturates, as is done in [6]. This can also be interpreted as how much the lateral force at the rear axle can be increased before the rear axle saturates. The static stability margin is similar to (19) defined as

$$\Gamma = 1 - \left| \frac{F_{Y2}}{D_{Y2}} \right| = 1 - \left| \frac{a_Y - (k^2/l_1)\ddot{\psi}}{\mu_2 g} \right| . \tag{20}$$

MMM Diagram and the Static Cornering Limits   The Milliken moment method diagram [12] is useful tool to visualize the grip margin, maneuverability and static stability margin metrics as is also done in [6]. The MMM diagram shows the lateral acceleration coefficient ($A_Y = a_Y/g$) on the horizontal axis and the yaw moment coefficient ($C_N = \ddot{\psi}k^2/(lg)$) on the vertical axis. The boundaries of the MMM diagram shown in Fig. 3.a are

11

determined by the grip of the front and rear axle. The diagonals which lie mainly in quadrants I and III mark the grip limit of the front axle. Likewise, the diagonals in quadrants II and IV mark the grip limit of the rear axle. The vertexes of the diagram naturally are where the lateral grip limit is reached on both the front and rear axle. Vertexes 1 and 3 are where the lateral forces maximize the lateral acceleration and have the same direction. At vertexes 2 and 4, the lateral forces have opposite signs and thereby give the maximum possible yaw moment. The boundaries of the diagram can be drawn through vertexes given by:

$$
\begin{aligned}
\mathbf{A}_Y &= (\begin{bmatrix} 1 & 1 & -1 & -1 \end{bmatrix}^{\mathrm{T}} D_{Y1} + \begin{bmatrix} 1 & -1 & -1 & 1 \end{bmatrix}^{\mathrm{T}} D_{Y2})/(mg) \\
&= (\begin{bmatrix} 1 & 1 & -1 & -1 \end{bmatrix}^{\mathrm{T}} l_2\mu_1 + \begin{bmatrix} 1 & -1 & -1 & 1 \end{bmatrix}^{\mathrm{T}} l_1\mu_2)/l \ , \quad (21) \\
\mathbf{C}_N &= (\begin{bmatrix} 1 & 1 & -1 & -1 \end{bmatrix}^{\mathrm{T}} l_1 D_{Y1} + \begin{bmatrix} -1 & 1 & 1 & -1 \end{bmatrix}^{\mathrm{T}} l_2 D_{Y2})/(lmg) \\
&= (\begin{bmatrix} 1 & 1 & -1 & -1 \end{bmatrix}^{\mathrm{T}} \mu_1 + \begin{bmatrix} -1 & 1 & 1 & -1 \end{bmatrix}^{\mathrm{T}} \mu_2)l_1 l_2/l^2 \ . \quad (22)
\end{aligned}
$$

For the case shown in Fig. 3.a $\mu_1 \geq \mu_2$ and the vehicle has a stable steady-state $(C_N = 0)$ limit when $\Xi = 0$ since that then $\Gamma \geq 0$.
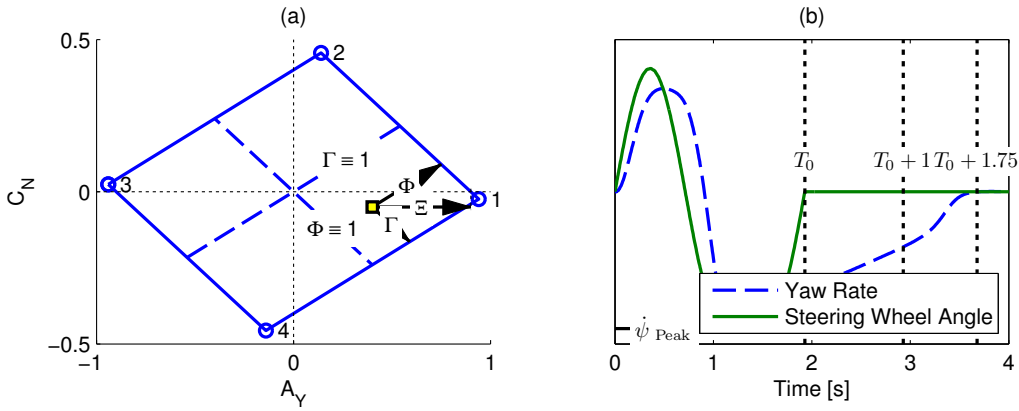
Figure 3: (a) Boundaries of an MMM diagram and an example of the lateral grip (Ξ), maneuverability (Φ) and stability (Γ) margins of an arbitrary point (marked with square) in the diagram. Additionally, the dashed lines indicate where the maneuverability and the static stability margins are 100%. (b) Steering wheel angle and yaw rate information used to assess stability according to FMVSS-126 [13].

5 Indicators of a Critical Cornering Situation

5.1 Indicators of Instability Utilizing Standard Sensor Data

In this subsection the focus is on indicators that are easily obtainable using wheel speed sensors (v_X), an angular rate sensor ($\dot{\psi}$), accelerometers (a_X and a_Y) and a steering wheel sensor (δ).

Yaw Rate Deviation The stability limit is assumed to be reached when the yaw rate error

$$\lambda_1 = e/\hat{\mu}, \tag{23}$$

is above a predetermined (negative) value. The scaling of the yaw rate error in (23) with the estimated friction from Sec. 3.5 is used to make the assessment of the yaw rate error more sensitive when the estimated friction is low.

Yaw Acceleration The large yaw moment which is a result of the steering reversal occurs approximately 1s. after the initiation of the maneuver can be detected via the yaw acceleration. As previously discussed, the yaw acceleration that is a result of the steering reversal is larger than what is possible by only steering in one direction.

What is evaluated is the following

$$\lambda_2 = |\ddot{\psi}|/\hat{\mu}, \tag{24}$$

which takes into account the estimated friction. In order to ensure a correct warning, the warning is only activated if the steering is out of phase with the lateral acceleration, i.e. $\delta a_Y < 0$. The yaw acceleration is estimated by differentiating the yaw rate sensor signal.

Side-Slip Rate Often, the side-slip of the vehicle is difficult to estimate, but the side-slip rate is easily computed from the yaw-rate, vehicle speed and lateral acceleration. Therefore another indicator that is evaluated is

$$\lambda_3 = |\dot{\beta}|/\hat{\mu}, \tag{25}$$

where

$$\dot{\beta} = \frac{v_X \dot{v}_Y - v_Y \dot{v}_X}{v_X^2 + v_Y^2} \approx \frac{\dot{v}_Y}{v_X} = \frac{a_Y - v_X \dot{\psi}}{v_X} \tag{26}$$

for small v_Y. The reason for choosing this indicator is that sustained high side-slip rate will eventually cause rear axle to saturate with loss of stability as a result.

5.2 Indicators of Instability Based on More Accurate Friction Estimation

There are numerous methods described in the literature on the topic of road friction estimation and a good summary on friction estimation methods can be found in [1]. If the friction would be more accurately known, two alternative approaches are proposed to estimate the lateral grip limit which will utilize the previously discussed stability, maneuverability and grip margins. The proposed indicators are

$$\lambda_4 = \Gamma - \Phi, \tag{27}$$

$$\lambda_5 = \Gamma - \Xi. \tag{28}$$

The reason for choosing these indicators is that the stability utilization (Γ) and maneuverability utilization (Φ) are closely related to the yaw acceleration. As previously discussed, excessive yaw acceleration is assumed to be an indication of a possible loss of stability. It was found that only using the stability or maneuverability margins do not produce an unambiguous threshold, which is why they are not separately used as indicators but in relation to the lateral grip utilization.

In the case of an accurate friction estimation, one could also study the derivative of the Lyapunov candidate (16). Using $\lambda_6 = \dot{V}$, it is not possible to guarantee the stability of the vehicle when $\lambda_6 > 0$.

6 Simulation Results

The sine-with-dwell maneuver [13] is evaluated on two different surfaces with the friction coefficient, μ_0, representing the surface condition. Additionally, the maneuvers were made with two different initial speeds. The steering amplitude is increased with discrete increments until the maneuver fails to meet the FMVSS 126 [13] stability requirement.

6.1 Warning Thresholds for Indicators λ_1 through λ_5

In Tab. 1 shows the maximum values for indicators λ_1 through λ_5, during a sine with dwell maneuver [13]. The thresholds are chosen such that for the indicators λ_1 through λ_5 exceeding the threshold will violate the requirements in (13), for Lyapunov stability (i.e. $\lambda_6 < 0$) and exponential stability (i.e. $|\psi t| < |g(t)|$). Violating these requirements is indicated with "NOK" in the table. The table shows that the threshold values are unambiguous for the two different surfaces. Since the threshold values need to be different for the

14

two speeds computed here, it is proposed to have the warning threshold to be speed dependent.

Name	Unit	80					120				
Initial speed	[km/h]	80					120				
FMVSS 126 stab,	[-]	OK	NOK	OK	NOK		OK	NOK	OK	NOK	
Steering Whl. Ampl.	[deg]	40	50	120	130		25	35	70	80	
Surface friction: μ_0	[-]	0,4	0,4	1	1		0,4	0,4	1	1	
		max, abs, values				thres-hold	max, abs, values				thres-hold
yaw rate error: e	[deg/s]	7,4	10,8	24,2	26,2	n/a	6,9	13,3	21,7	29,3	n/a
$e / \hat{\mu} = \lambda_1$	[deg/s]	19,9	28,8	26,0	28,2	24,9	20,0	37,9	23,9	31,8	28,4
yaw acceleration: $\ddot{\psi}$	[deg/s/s]	74	89	226	242	n/a	47	59	141	153	n/a
$\ddot{\psi} / \hat{\mu} = \lambda_2$	[deg/s/s]	233	260	251	265	247	149	170	156	166	161
side-slip rate: $\dot{\beta}$	[deg/s]	8,1	10,6	22,4	24,2	n/a	8,9	12,3	25,3	28,5	n/a
$\dot{\beta} / \hat{\mu} = \lambda_3$	[deg/s]	25,7	31,1	24,8	26,6	24,8	28,2	35,1	28,1	31,0	30,6
$\Gamma - \Phi = \lambda_4$	[-]	1,034	1,068	1,052	1,058	1,060	0,718	0,816	0,755	0,800	0,772
$\Gamma - \Xi = \lambda_5$	[-]	0,676	0,754	0,726	0,768	0,719	0,431	0,492	0,453	0,480	0,464

Table 1: Maximum values for different indicators during a Sine with Dwell maneuver [13] for two different surfaces and on two different initial speeds. The dark green/gray fields are the two indicator values which are closest to the threshold (the threshold value for each speed) in (13). The light green/gray values are those that are on the right side of the threshold value. Any indicators on the wrong side of the threshold would have been marked seperately.

6.2   Evaluation of Warning Indicators

In Fig. 4.a and 4.b it can be seen that the warning indicators λ_2 through λ_5 give a warning closely following the steering reversal. The warning indicators λ_1 and λ_6 shown in Fig. 4.a and 4.c exceed their threshold value only after the steering maneuver is completed. By comparing Fig. 4.a and Fig. 4.d it can be seen that λ_4 and λ_5 are good indicators of the instability caused by the steering reversal during the sine-with-dwell maneuver. These indicators peak as the trajectory shown in Fig. 4.b crosses the lines where $\Phi = 1$ and $\Xi = 1$. As discussed in Sec. 4, knowing the surface friction and having computed the contours of Lyapunov surface gradient will allow us to assess the stability of the maneuver using the gradient of a Lyapunov candidate function. In Fig. 4.d, the solution which violates the thresholds in Tab. 1 for the indicators λ_1 through λ_5 also crosses the contour where $\dot{V} = 0$.

Our conclusion is that the λ_2 and λ_3 indicators which are based on the yaw acceleration and side-slip rate, respectively, are the most suitable early

15

indicators of yaw instability. In favor of these indicators, over for instance λ_4 and λ_5, is also that λ_2 and λ_3 only rely on a crude estimation of the surface friction.

6.3   Post-Maneuver Stabilization

As can be seen in Fig. 4, the warnings related to the yaw acceleration (λ_2, λ_4 and λ_5) and the side-slip rate (λ_3) all give the driver nearly one second to react after the completion of the maneuver. The proposed driver action is a one second countersteer maneuver as can be seen in Fig. 5.c. Four different stabilizing strategies are here evaluated:

1. no countersteer and without ESC (reference);

2. no countersteer with only ESC intervention;

3. countersteer sufficient to stabilize the vehicle without ESC (ESC off);

4. countersteer, combined ESC and countersteer.

The results of these different stabilizing strategies are shown in Fig. 5. It can be seen in Fig. 5.a and 5.c that all four stabilization strategies work with the countersteer well within the capability of most drivers [3]. It can be seen in Fig. 5.b that when the countersteer is combined with ESC control (iv), the ESC is activated earlier and with less intensity than when the driver does not countersteer (ii).

7   Conclusions and Future Work

In this paper several indicators of instability are reviewed during a lane-change type maneuver. The lane-change type maneuver used here is the sine-with-dwell maneuver from the FMVSS-126 regulation [13]. The maneuver was suitable for our purpose of evaluating stability, since the maneuver is designed to invoke vehicle instability and thereby evaluating the ESC system's effectiveness to stabilize the vehicle. It was here assumed that it would be beneficial if the driver could cooperate with the ESC system by countersteering after the completion of the lane-change maneuver. For this purpose several indicators related to for instance the yaw acceleration and the side-slip rate together with a crude friction estimation were developed. These were shown to give unambiguous warning thresholds on the two different surface for which these indicators were evaluated. Additionally, these indicators could trigger a warning for which the driver would have around one
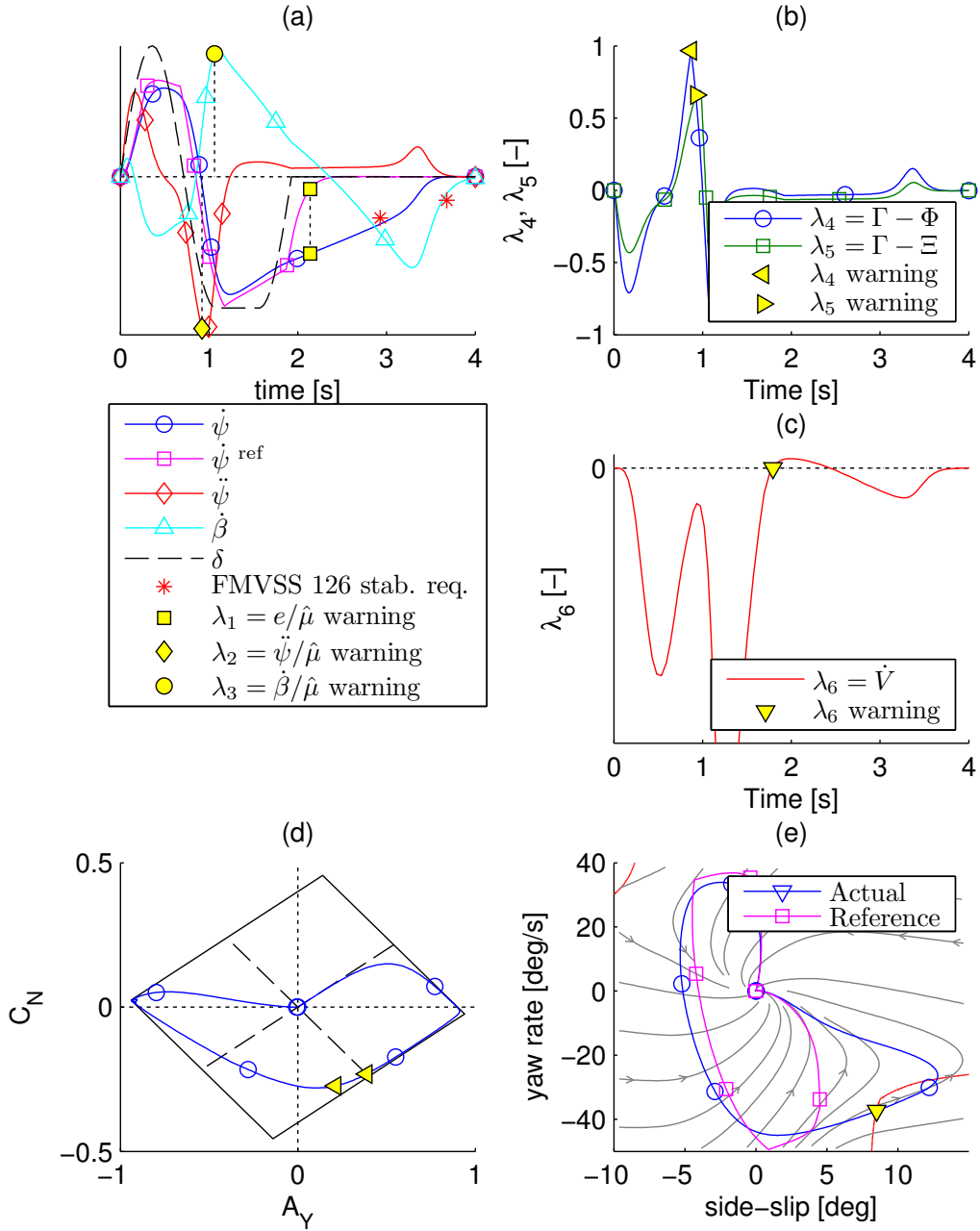
Figure 4: Results from a sine-with-dwell maneuver with a steering wheel amplitude of 130°, an initial speed of 80km/h on a dry surface ($\mu_0 = 1$). Warnings are based in (a) on a crude friction estimation. In (b) warning indicators are based on safety margins and compared in (d) to the MMM diagram limits and A_Y and C_N for the maneuver. In (c) the derivative of the Lyapunov candidate function for the maneuver; and (e) a phase portrait with the a contour (solid lines without markers or arrow) of the Lyapunov gradient where $\dot{V} = 0$ and the states of the actual and reference vehicle models.
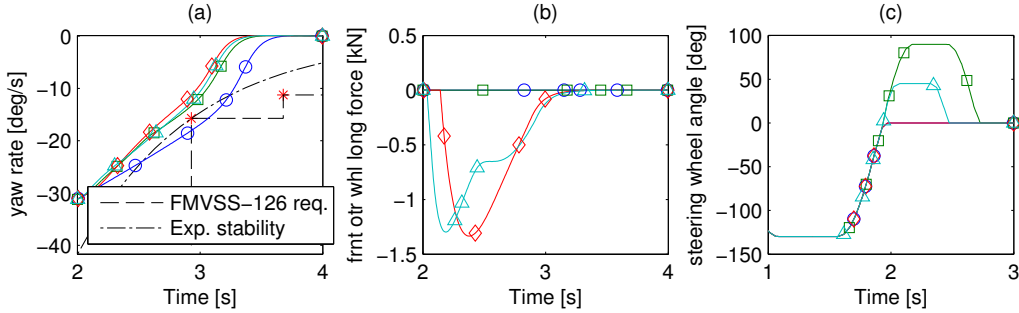
Figure 5: Results a sine-with dwell test with different post-maneuver stabilizing strategies. As in Fig. 4 the asterisks in (a) define the limits defined in [13] to which the yaw rate must have decayed after $t = 1$ and $t = 1.75$ seconds after completion of the maneuver, respectively. For both sub-figures, the results from the strategies are marked with (i) a circle for $\delta_{cs} = 0°$ with ESC off, (ii) a square $\delta_{cs} = 90°$ with ESC off, (iii) a diamond for $\delta_{cs} = 0$ with ESC on and (iv) a triangle for $\delta_{cs} = 60°$ with ESC on.

second to take corrective action. These indicators, which were based on easily measurable variables, were further compared to classical evaluation tools such as the MMM diagram [12], phase portrait analysis and Lyapunov stability [7]. The conclusions are that stability indicators based on side-slip rate and yaw acceleration give an early indication of possible instability. Other methods such as the Lyapunov analysis and deviation from a reference model gave an indication of instability only after completion of the maneuver. Although these other indicators gave unambiguous results, which is meant to say that these indicators did not give false positive of false negative warnings, the warning comes too late to be useful for driver warning. Rather than using it for driver warning, the deviation from a reference model was used to trigger the ESC system which brakes the individual wheels to stabilize the vehicle. It was shown that a combination of countersteer and ESC intervention triggered a quicker ESC intervention with a shorter duration. This is understood to show that a cooperation between the driver and the stability control gives a better overall system performance. For completeness, future work should include different concepts for how to warn the driver which may be triggered based on the indicators in this work. It would also be necessary to evaluate these warning strategies using a study with real drivers, likely using a vehicle simulator.

18

Acknowledgments

References

[1] M. Andersson, F. Bruzelius, J. Casselgren, M. Gäfvert, M. Hjort, J. Hulten, F. Habring, M. Klomp, G. Olsson, M. Sjödahl, J. Svendenius, S. Woxneryd, and B. Wälivaara. Road friction estimation. Technical report, IVSS Project Report 2004:17750, 2007.

[2] C. Bielaczek, M. Barz, B. Breuer, W. Rohmert, and J. Breuer. Development of warning strategies and driver-vehicle interfaces. In *Conference for Enhanced Safety of Vehicles (ESV)*, 1996.

[3] G. J. Forkenbrock and D. Elsasser. An assessment of human driver steering capability. Technical report, NHSTA DOT HS 809 875, 2005.

[4] Y. A. Ghoneim, W. C. Lin, D. M. Sidlosky, H. H. Chen, Y.-K. Chin, and M. J. Tedrake. Integrated chassis control system to enhance vehicle stability. *International Journal of Vehicle Design*, 23:124–144, 2000.

[5] M. Hiemer. *Model Based Detection and Reconstruction of Road Traffic Accidents*. PhD thesis, Universität Karlsruhe, Fakultät für Elektrotechnik und Informationstechnik, 2004.

[6] R. C. Hoffman, J. L. Stein, L. S. Louca, and K. Huh. Using the Milliken Moment Method and dynamic simulation to evaluate vehicle stability and controllability. *International Journal of Vehicle Design*, 48(1-2):132–148, November 2008.

[7] H. Khahil. *Nonlinear Systems*. Prentice Hall, New Jersey, third edition edition, 2002.

[8] M. Klomp. *On Drive Force Distribution and Road Vehicle Handling – A Study of Understeer and Lateral Grip*. Licentiate Thesis, Chalmers University of Technology, 2007.

[9] A. S. Krausman, R. A. Pettitt, and L. R. Elliott. Effects of redundant alerts on platoon leader performance and decision making. Technical report, US Army Research Laboratory, 2007.

[10] A. Linder, T. Dukic, M. Hjort, Y. Mastoms, S. Mardh, J. Sundström, A. Vadeby, M. Wiklund, and J. Östlund. Methods for the evaluation of traffic safety effects of antilock braking system (ABS) and electronic stability control (ESC) – a literature review. Technical report, VTI report 580A, 2007.

[11] J. Lu, D. Filev, K. Prakah-Asante, F. Tseng, and I. V. Kolmanovsky. From vehicle stability control to intelligent personal minder: Real-time vehicle handling limit warning and driver style characterization. In *IEEE Symposium on Computational Intelligence*, 2009.

[12] W. F. Milliken and D. L. Milliken. *Race Car Vehicle Dynamics*. SAE International, 1995. 1-56091-526-9.

[13] NHSTA. Laboratory test procedure for fmvss 126, electronic stability control systems. In *TP126-02*, 2008.

[14] H. B. Pacejka. *Tyre and Vehicle Dynamics*. Butterworth-Heinemann, Oxford, UK, 2 edition, 2006.

[15] V. K. Sadekar, D. K. Grimm, B. B. Litkouhi, and R. J. Kiefer. An integrated auditory warning approach for driver assistance and active safety system. In *SAE Technical Paper 2007-01-0443*, 2007.

[16] SAE. Road/lane departure warning systems: Information for the human interface. In *SAE Technical Standard J2808*, number J2808, 08 2007.

[17] K. Suzuki and H. Jansson. An analysis of driver's steering behaviour during auditory or haptic warnings for the designing of lane departure warning system. *JSAE Review*, 24:65–70, 2003.

[18] A. T. van Zanten. Bosch esp systems: 5 years of experience. In *SAE Technical Paper 2000-01-1633*, 2000.

[19] H.-P. Willumeit, M. Neculau, A. Vikas, and A. Wöhler. Mathematical models for the computation of vehicle dynamic behaviour during development. In *Proceedings of the 24th FISITA Congress*, 1992.

A Vehicle and Tire Data

In this work, a simplified version of the well-known Magic tire model [14] which use the longitudinal force F_X and the slip angle α as independent variables. The Magic tire formula coefficients which are used here are

$$D_{ij} = \sqrt{(\mu_0 \mu_i F_{Zij})^2 - F_{Xij}^2}, \quad C = 4/3, \quad B = 10/\mu_0, \quad E = -2, \qquad (29)$$

where $i = 1, 2$ and $j = 1, 2$ are for the front/rear axle and left/right wheels, respectively.

The vehicle data shown in Tab. 2 that are used in the conducted simulations represent a medium-sized passenger vehicle.

Description	Symbol	Unit	Value
Vehicle mass	m	[kg]	1675
Yaw radius of gyration	k	[m]	1.32
Wheel base	l	[m]	2.675
Distance of front axle to mass center	l_1	[m]	$l/5$
Height of mass center	h	[m]	0.5
Front and rear track width	w	[m]	1.5
Front/rear axle lateral load transfer coefficient	ζ_1/ζ_2	[-]	0.17/0.16
Front/rear axle tire/road friction	μ_1/μ_2	[-]	0.9/1.0
Front area	A_f	[m^2]	2.14
Aerodynamic drag coefficient	C_D	[-]	0.30
Tire rolling resistance	σ	[-]	0.010
Tire radius	R	[m]	0.32

Table 2: Vehicle Dimensions